Acta Materialia 208 (2021) 116706

Contents lists available at ScienceDirect

Acta Materialia

journal homepage: www.elsevier.com/locate/actamat

Role of tantalum concentration, processing temperature, and strain-rate on the mechanical behavior of copper-tantalum alloys

S. Srinivasan[a], S. Sharma[a], S. Turnage[a,b], B.C. Hornbuckle[b], C. Kale[a], K.A. Darling[b], K. Solanki[a,*]

[a] School for the Engineering of Matter, Transport, and Energy, Arizona State University, Tempe, AZ 85287, United States
[b] Army Research Laboratory, Weapons and Materials Research Directoratetate APG, MD 21014, United States

ARTICLE INFO

Article history:
Received 14 May 2020
Revised 20 January 2021
Accepted 27 January 2021
Available online 1 February 2021

Keywords:
Nanocrystalline
Strain rate
Flow stress upturn
Microstructure

ABSTRACT

Microstructural instability in traditional nanocrystalline metals limits the understanding of the fundamental effect of grain size on mechanical behavior under extreme environmental conditions such as high temperature and loading rates. In this work, the interplay between Ta concentrations and processing temperature on the resulting microstructure of a powder processed, fully dense Cu-Ta alloy along with their tensile and compressive behavior at different strain rates are investigated to probe the possibility of manipulating or tuning microstructurally dependent parameters to control the flow-stress upturn phenomenon. Consequently, the results reveal that there is a crucial length scale, i.e., small grain size and appropriate cluster spacing, below which such upturn is damped out. The observation of changes in flow stress upturn behavior is consistent with the observed changes in measured high-rate plasticity, which enhances below the critical length scale. Furthermore, tension-compression asymmetry also tends to be suppressed in nanocrystalline Cu-Ta alloys, while it becomes evident as the grain size increases to an ultrafine regime. Overall, this work presents a systematic approach to control or engineer reduced high strain rate flow stress upturn behavior in metallic alloys, for high-rate applications.

1. Introduction

Under a uniaxial state of stress as the rate of loading is increased to a critical point (~10^4 s^{-1}), most metals undergo a rapid up-turn in their flow stress [1]. Such flow stress transition varies for different materials [1], and the strength increases by several 100% as the rate of deformation is increased [2–5]. For instance, at room temperature, Follansbee et al. [6] experimentally observed the flow stress upturn in oxygen-free high conductivity (OFHC), face-centered cubic (FCC) copper to be increased by six times at ~4.0×10^3 s^{-1} as compared to the quasi-static condition. Likewise, for similarly applied strain rates in coarse-grained nickel, the flow stress was found to experience approximately a 55% increase compared to its quasi-static flow stress [5]. Though the exact mechanism of such transition has not been established, it has been often associated with the transition from thermally activated dislocation motion to drag-dominated dislocation motion, largely brought about by interactions with phonons within the lattice [1,7]. In other words, the drag stress, τ_d, contribution to dislocation motion becomes significant as the deformation rate is increased [1], i.e., $\tau_d = Bv/b$, where B is the drag coefficient, which is a function of temperature, b is the Burgers vector, and v is the dislocation velocity. Furthermore, variation in the amount of increase in the flow stress at high strain rates has also been attributed to the effective mass of dislocation under acceleration, and its interaction with microstructural features (e.g. grain boundaries and precipitates), both of which are dependent on the applied temperature [8]. However, such propositions and theories were mostly made based on atomistic simulations and modeling, since gaining experimental evidence for phenomena such as phonon drag is relatively difficult [9,10]. Recently, Lea et al. have experimentally demonstrated that the flow stress upturn in polycrystalline materials is driven mainly by another mechanism involving the self-organization of dislocations [11]. That is, in conventional polycrystalline materials where plasticity is mediated through self-organization of dislocation /avalanche dislocation (referred to as self-organized criticality/SOCs), maintaining such self-organization at a high strain rate is constrained by the time available, resulting in multiple short dislocations instead, causing the high-rate strengthening. Altogether, in both the theories: phonon drag effect and time limiting SOCs, the flow stress upturn is controlled mainly by the changes in dislocation structure and behavior at high rates compared to the quasi-static conditions.

* Corresponding author.
E-mail address: kiran.solanki@asu.edu (K. Solanki).

https://doi.org/10.1016/j.actamat.2021.116706
1359-6454/

Thus, if the material microstructure characteristics can be tailored to control the dislocation activity, it provides a convenient avenue for controlling flow stress upturn behavior at a high strain rate. That is, the perturbations of a moving dislocation caused by interacting with microstructural features can be used to alter the manifestation of the flow stress upturn in a material. Unfortunately, in most crystalline materials, the available mean free glide path between microstructural features/perturbations is too large to restrict dislocation self-organization or the average dislocation velocity below the inherent threshold required for phonon drag effects. For instance, a moving dislocation in Cu requires only ~15 nm to accelerate to a steady-state velocity [12]. So, while there has been some degree of manipulation of the flow stress upturn based on the high-rate acceleration of dislocations, traditional microstructural length-scales have not been sufficient to provide damping out of the phonon drag effect or the time limiting self-organized criticality (SOCs or the avalanche dislocations). Alternatively, it may be hypothesized that if the mean free path between microstructural features could be stabilized below a certain point, phonon drag can be constricted owing to the inability to attain that critical velocity, and similarly, the SOCs will lose their role in flow stress upturn since the spatial limit is constrained to enable their formation even at nominal strain rates. For instance, recent work by Turnage et al. [12] and Casem et al. [13] on microstructurally stable NC-Cu-10at.%Ta showed negligible changes in the room temperature compressive flow stress up to 10^7 s^{-1}, i.e., no flow stress up-turn. This is unlike the increased strain rate sensitivity observed in literature for certain nanocrystalline metals compared to their coarse-grained counterparts [14]. For instance, conventional pure NC Ni was reported to present a 70% increase in the flow stress at 10^3 s^{-1}, as compared to its flow stress at 10^{-3} s^{-1} [5]. Such high upturn and similar ones exhibited by coarse-grained pure Cu at 298 K was observed only at a high homologous temperature (0.55 T_m) in NC-Cu-10at.%Ta as reported by Turnage et al. [12]. It was suggested that the initial mechanism for such behavior was related to a reduced dislocation velocity associated with damping out through a pinning interaction with a critical length scale of stable atomic clusters. As the drag coefficient has temperature dependence, this mechanism was ultimately overcome through the application of high homologous temperatures. Such divergent experimental results (NC Ni and NC Cu-Ta) point to the need for a systematic methodology to determine the role of microstructural features and subsequent critical length on the dislocation interactions controlling the flow stress upturn. Thus, we take a different approach by manipulating or tuning microstructural dependent parameters to control the same upturn phenomenon. In this regard, alloys with different solute compositions and processing temperatures were used to systematically study the role played by grain size, Ta nanoclusters, and other microstructural parameters on the increase in the flow stress as a function of strain rate in both tension and compression.

2. Experimental methods

2.1. Powder processing

To distinguish between the effects that grain boundaries and Ta nanoclusters have on tensile ductility, strength, and strain rates at which flow stress upturn occurs, five different compositions of a Cu-Ta alloy, namely Cu-0.5at.%Ta, Cu-1at.%Ta, Cu-3at.%Ta, Cu-5at.%Ta, and Cu-10at.%Ta were synthesized. Initially, powders were processed using mechanical alloying at cryogenic temperatures followed by equal channel angular extrusion (ECAE) at temperatures of 700°C, 900°C, and 1000°C. Processing parameters follow the procedures outlined in [15,16], where elemental powders of Cu and Ta mixed under argon atmosphere in the correct proportions are loaded 10 g at a time into a 440C stainless steel vial with 440C stainless steel milling media and milled for 4 hours at liquid nitrogen temperatures. After milling, powders from separate milling batches were combined and thoroughly mixed; afterward, they were loaded into Ni cans sealed under argon. These powder-filled cans were then heated to the processing temperature and extruded through an angle of 90° generating fully dense billets of material. By varying compositions at similar processing temperatures, the effects of Ta nanoclusters can be investigated with limited influence from differences in grain size; whereas, varying processing temperatures allow the analysis of the effects of grain size with limited influence of varying Ta nanoclusters.

2.2. Quasi-static and high-rate testing

Upon consolidation into a bulk form, samples for tensile and compressive testing were cut along the extrusion direction of the billets in the form of rectangular dog-bone tensile specimens and 3 mm in diameter by 3 mm in length cylindrical compression specimens [17]. Quasi-static tensile/compressive tests at various strain rates were performed with an electromechanical universal testing machine equipped with an extensometer and corrected to reveal true stress-true strain results. High strain rate tests were conducted using the Kolsky bar technique described in [18–20] but with specialized grips for the tension to accommodate the rectangular dog-bone specimens. Both the bar and the grips were made from Inconel 718. For the tensile test, a striker tube of equal mechanical impedance to the incident and transmitted bars impacts a flange on the incident bar causing a tensile pulse to be generated which travels to the specimen. For the compression testing, the striker bar impacts the incident bar generating a strain pulse that travels to the specimen, which is held in place between the incident and transmitted bars. In both cases, as the pulse impacts the specimen, part of the pulse is transmitted through the specimen to the transmitted bar, where strain gauges in a Wheatstone bridge configuration are used to measure the force traveling through the specimen. The remainder of the pulse is reflected back toward the strain gauges on the incident bar which provides information on the strain experienced by the sample (refer to [12,19–21]). The strain rates of Kolsky bar testing in this work were around 10^3 s^{-1} and for the tensile test, the samples were strained until failure. For the compression high rate testing, the flow stress was taken at a 10% strain level. In the case of tension, due to limitation on measured stress-strain responses, particularly at high strain-rates, flow stress (~yield stress) at 0.2% strain was calculated to understand strain rate sensitivity behavior. It is well known that due to the time required for a sample to reach force equilibrium across the specimen, the flow stresses measured on a Kolsky bar should be carried out at higher strain levels where equilibrium is attained. However, it should be noted that the normalized flow stress at 0.2% strain in tension is just a qualitative comparison of how much of an increase in yield stress could be observed because of the higher strain rate deformation for different microstructure, and the trend is validated through complementary compression experiments where the samples exhibit higher strain values. Furthermore, it will be shown that the material does not exhibit enough strain hardening (relatively elastic-perfectly plastic) and the high strain rate behavior at different strain levels in compression, as well as 0.2% in tension versus 10% in compression, are comparable.

2.3. Microstructural characterization

Samples for TEM characterization were lifted out from the region close to the fracture surface using a Focused Ion beam (FIB) FEI Nova 500 and eventually thinned to electron transparency.

Table 1
The initial grain size of Cu-Ta alloys processed at various temperatures.

Ta at. %	Processing T (°C)	Initial grain size (nm)
Cu 0.5 at.% Ta	700	600
Cu 1 at.% Ta	700	168
	900	283
	1000	1200
Cu 3 at.% Ta	700	99
Cu 5 at.% Ta	700	82
	900	201
	1000	500
Cu 10 at.% Ta	700	50
	900	213
	1000	500

The lamella was then plasma cleaned in an argon atmosphere for ~15-20 mins. Multiple bright-field (BF) and dark-field STEM images were captured at various magnifications using the aberration-corrected ARM 200F (JEOL) to assess the microstructure, such as grain size and nanoclusters, in the as-received as well as deformed specimens. More than 200 grains were sampled to generate an average grain size for each condition using ImageJ software.

3. Results and discussions

3.1. As-received Microstructure

Table 1 shows consistent trends within the data, which are as solute concentrations were decreased and/or processing temperature increased the average grain size for any given alloy, increases. By manipulating these parameters, we can generate a range of grain sizes from 50 to 1200 nm as listed in Table 1. By having such a range in the microstructure, we can then probe the effects the deformation rate has relative to the microstructure.

Fig. 1 shows the microstructure for Cu-1at.%Ta and Cu-5at.%Ta processed at 700 and 900°C to depict the trend in Table 1. It should be noted the higher solute content in Cu-5at.%Ta does result in the bimodal size distribution of Ta particles with smaller clusters (average diameter of 3 nm) and larger particles (average diameter of 30 nm). This distribution holds true in Cu-10at.%Ta as well, while Cu-0.5at.%Ta, Cu-1at.%Ta, and Cu-3at.%Ta (Refer [22] for the 3% microstructure) mainly contain the finer clusters due to the restricted solute content. This also speaks to the solubility limit of Ta in Cu, and the ability of high energy mechanical alloying to extend the thermodynamic constraints of the system by solutionizing ~ 3 at% Ta within the Cu lattice. When considering the finer Ta clusters, earlier atom probe studies on Cu-1at.%Ta and Cu-10at.%Ta showed a Ta cluster density of about 4.1×10^{23} m^{-3} and 6.5×10^{23} m^{-3}, respectively, and cluster spacing on the order of 5-15 nm [16]. These changes in spacing and cluster density could play a critical role as it will be discussed later in terms of the dislocation velocity and their effects on the strain rate sensitivity. Furthermore, the alloys with higher Ta concentration and nanocrystalline microstructure do not seem to possess avalanche dislocations or the self-organized criticality (SOCs) in their microstructure since the spatial limit for their formation is constrained by numerous densely spaced obstacles (precipitates and grain boundaries). Thus, flow stress upturn in such alloys could be contributed from the other phonon drag mechanism which also needs to be suppressed to control the flow stress upturn.

3.2. Role of average grain size and Ta nanocluster spacing on the flow stress upturn

After processing various samples that exhibit different average grain sizes and inherently varying Ta nanocluster density/spacing, tensile and compression tests were carried out at various strain rates. The true stress-strain responses of various Cu-Ta alloys in tension (Fig. 2A-B) and compression (Fig. 2C-D) revealed unique distinctions between the NC and the ultrafine-grained specimens. At quasi-static strain rates, the alloys processed at 700 °C, i.e., those with the smallest grain size, (i.e. 5-10 at% Ta concentration) exhibited an extremely high yield strength and brittle behavior in tension failing at the end of the elastic region, while the larger grained samples experienced enhanced plasticity between approximately 5% and 10%. For instance, Cu-10at.%Ta processed at 700°C possesses yield strength of almost 1.1 GPa (however, failed before reaching its true yield value based on compression data), which decreased to 645 and 530 MPa when increasing the processing temperature to 900°C and 1000°C (increasing grain size), respectively. At similar processing temperatures, alloys with higher Ta content possess higher yield strength as expected. Interestingly, Cu-3at.%Ta demonstrated a similar 0.2% compressive flow stress compared to 5 and 10at.%Ta, even though the microstructure of the Cu-3at.%Ta alloy contained a negligible amount of larger (30-60 nm) incoherent Ta based particles. However, the 3% alloy has approximately the same number density of the smaller, coherent/semi-coherent Ta based nanoclusters [[16]]. Over the entire strain-rates range, the compression true stress-strain responses displayed an elastic- nearly perfectly plastic behavior with no significant strain hardening. To understand the role of Ta, Fig. 2C compares alloys with various Ta concentrations keeping the processing temperature the same. Very little strain rate sensitivity was apparent for Cu with 3, 5, and 10at.%Ta processed at 700°C; however, significant rate effects were observed for a Cu-0.5at.%Ta alloy as seen in Fig. 2C. Furthermore, at high strain rates, the larger grained samples experienced higher flow stress and a loss of tensile ductility as compared to their corresponding values at quasi-static strain rates. This is a typical response of generic coarse-grained material during a high strain rate test, i.e., in a large-grained metal, lattice dislocations can achieve steady-state velocity, thereby bring the effect of phonon drag (increase in the τ_d contribution). However, nanocrystalline alloys like Cu-10at.%Ta samples processed at 700°C, which has the smallest grain size (50 nm), experienced a relatively low increase in the flow stress and enhanced plasticity at higher strain rates. This is unlike the response expected in a typical coarse-grained metal [1]. This behavior is shown in Fig. 2D where Cu-10at.%Ta samples processed at 900 and 1000°C show a much higher increase in flow stress at a high strain rate compared to that at 700°C. Refer to appendix Fig. A1 for compression curves of other alloy concentrations and processing temperatures.

To further elucidate the effect of strain rate on the flow stress of various Cu-Ta microstructures, first, the high tensile strain rate 0.2% flow stress was normalized with the corresponding quasi-static strain rate stress for the same material and condition. For the compression behavior, the flow stress values were taken for each strain rate at 10% plastic strain. Fig. 3 shows the normalized flow stress as a function of strain rate and grain size for each specimen and conditions. As mentioned earlier, it should be remembered that the normalized flow stress in tension is a qualitative comparison measure of how much of an increase in yield stress could be observed because of the higher strain rate deformation for different microstructure, and the trend is consistent with complementary compression experiments where the samples exhibit higher strain values. That is, for the tension data, despite taking stress values from correspondingly low strain, where questions of attaining equilibrium during testing may arise, the correlations made are consistent with compression, where these concerns do not exist.

As such, the results (Fig. 3) revealed that alloys with both NC grain size and moderate to high Ta concentrations exhibited the

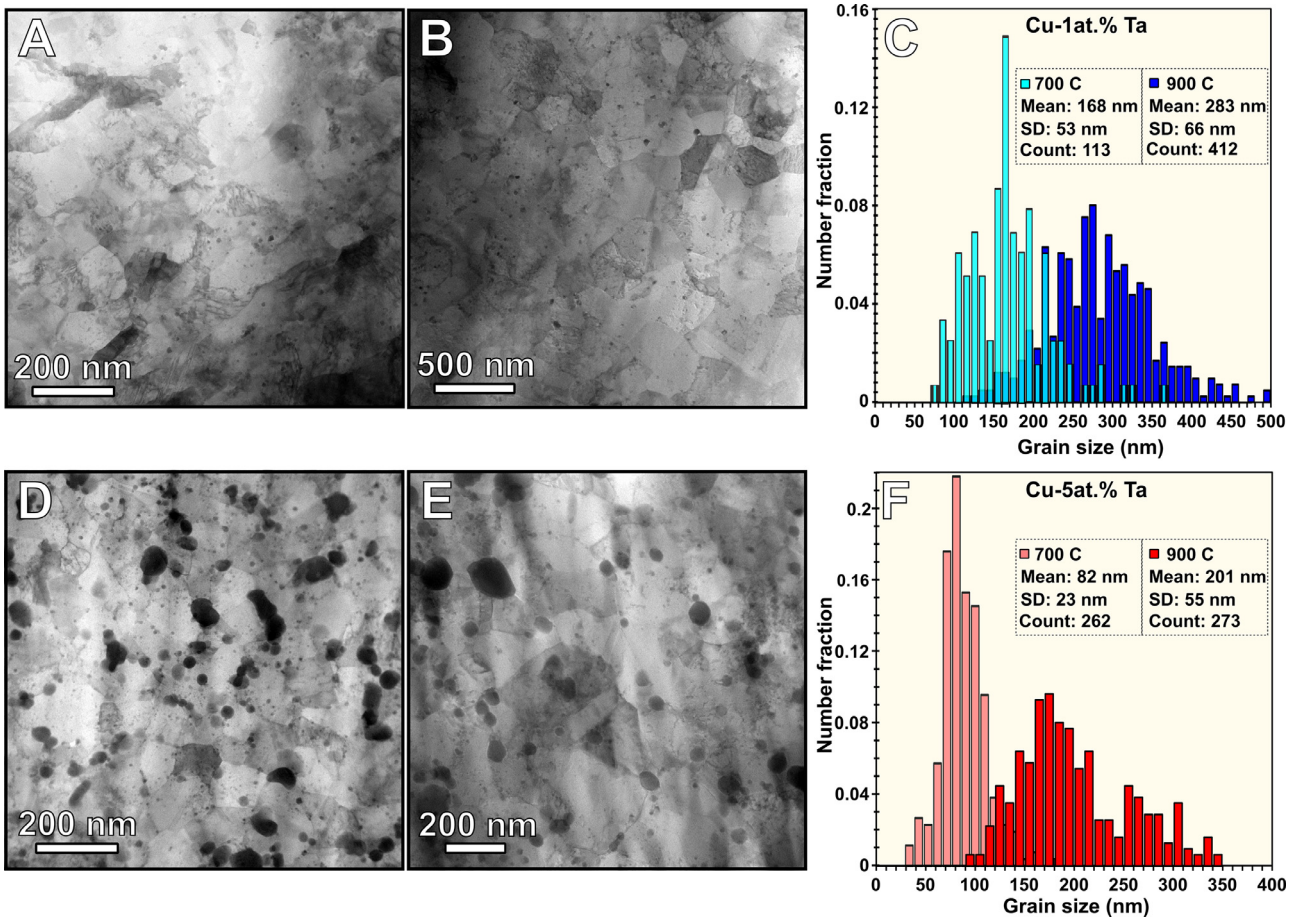

Fig. 1. As- received BF STEM micrographs and grain size statistics for (A-C) Cu-1at.%Ta processed at 700°C and 900°C, (D-E) Cu-5at.%Ta processed at 700°C and 900°C respectively.

lowest rise in flow stress, as the strain rate (tensile or compressive) was increased. Further, for each concentration, as processing temperature increased causing grain size to increase, the normalized flow stress also increased. This indicates the importance of grain boundaries in dislocation nucleation and pinning. Interestingly, though Cu-10at.%Ta processed at 900°C has a slightly larger grain size than the Cu-1at.%Ta processed at 700°C, the rise in flow stress was greater for the Cu-1at.%Ta processed at 700°C indicating the role Ta nanoclusters play in limiting the effects of dislocation drag in addition to the grain size at higher Ta concentration. Furthermore, consistent with the previous work [23], the tension-compression asymmetry was also suppressed in Cu-10at.%Ta processed at 700°C and other alloys that possess nanocrystalline grain size. However, as the processing temperature (grain size) increased and the Ta concentration decreased, tension-compression asymmetry became evident as seen from plots A and B in Fig. 3, where the magnitude of flow stress increase is higher in tension compared to compression in coarse-grained alloys. Such an asymmetry was not reported before by the authors, as dynamic deformation studies were limited to nanograined Cu-Ta alloys only. Additionally, to compare the effects of strain hardening on the flow stress upturn, a comparison of flow stress values taken from different strain levels between tension and compression are included in Appendix, which shows a consistent trend (up-turn) for different strain-level or tension versus compression for various Cu-Ta alloys. Overall, the data presented in Fig. 3 illustrates the importance of controlling/tuning grain size and Ta nanocluster spacing on the flow stress behavior.

3.3. Post deformation microstructure

To gain more insights into the observed deformation behavior, we next focus on understanding the microstructural changes upon deformation. In our previous work on compression behavior, it has been shown that Ta nanocluster size and spacing do not change with respect to various thermo-mechanical loading conditions [12,15,16,23–26]. Note that Turnage et al. [12] and Kale et al. [25] have discussed in detail the post-deformed microstructure in compression. With that in mind, we focused on evaluating changes in grain size and dislocation activities in tension. Fig. 4 shows the post tensile microstructure of Cu-1at.%Ta and Cu-5at.%Ta processed at 700°C quasi-static and high strain rate conditions. After deformation at both rates, there was no significant grain growth observed in Cu-5at.%Ta alloy when compared to the as-received (average grain size of 82 nm) condition. Similarly, the Cu-1at.%Ta alloy experienced a small amount of grain growth after deformation at both quasi-static and high rates (~226 nm) as compared to the as-received (grain size of 168 nm) condition. These small changes in the microstructures, i.e., slight increase in the grain size upon deformation, could be related to variation in the number density of Ta nanoclusters that are initially pinning the grain boundary. In our earlier atomistic work, it was shown through the Zener model that the minimum grain boundary area per cluster (~density) is on the order of 4.84 nm^2 [26], and any variation in this number could lead to zipping and unzipping of grain boundary during deformation. Furthermore, significant dislocation bursts in multiple grains were observed in Cu-1at.%Ta (Fig. 4A, A') as compared to

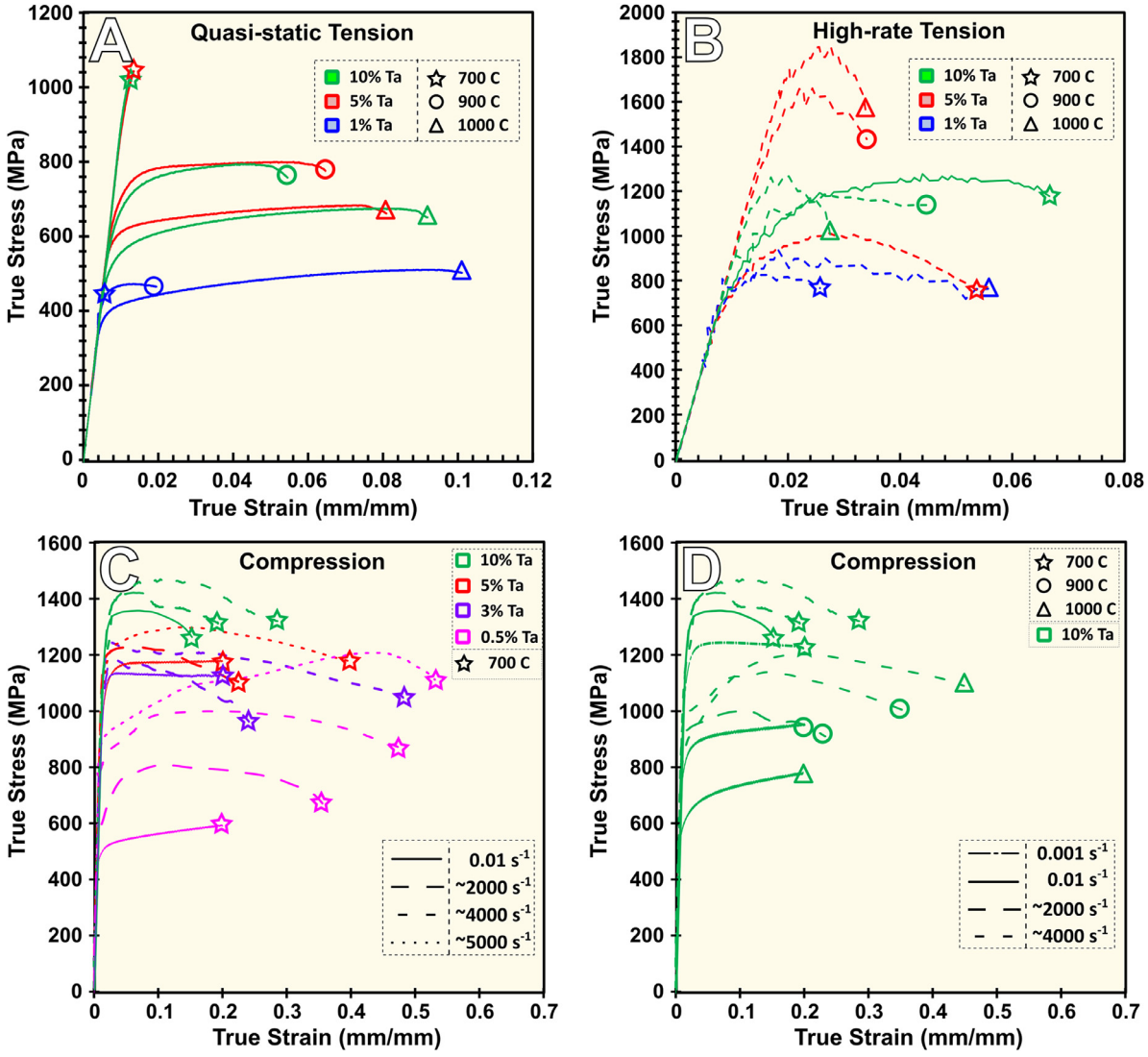

Fig. 2. Stress-strain response for the various samples in (A&B) Tension at quasi-static and high strain rates respectively and (C) Compression curves at various strain rates comparing all alloys processed at 700°C (D) Compression curves at various strain rates comparing 10%Ta alloy processed at 700, 900 and 1000°C. Other curves are included in the appendix. Solid lines correspond to quasi-static strain rates while dashed lines correspond to high strain rate tests. The Ta concentrations are color-coded with pink, blue, purple, red, and green corresponding to concentrations of 0.5 at.%, 1at.%, 3 at.%, 5 at.%, and 10at.%, respectively. The markers at the point of failure for each sample are denoted by the ☆, O, and Δ which correspond to samples processed at 700°C, 900°C, and 1000°C, respectively.

Cu-5at.%Ta (Fig. 4C, C') under quasi-static conditions, highlighted with yellow arrows. Moreover in the ultra-fine grained Cu-1at.%Ta multiple dislocations appeared to be clustered within the grain, propagating from one end to the other of the grain boundary owing to limited density of obstacles (Ta nanoclusters/grain boundaries) to constrain them. Whereas in Cu-5at.%Ta, which has a grain size in the NC regime (82 nm), at a high rate, most of the dislocations were observed to be pinned at nanoclusters (highlighted in 4 C' and D') or grain boundaries, limiting the dislocation propagation (line length) and pile-up (self-organization). This is very important since plastic deformation is governed by the mobile dislocation density and the average mobile dislocation velocity, which in turn controls the SOC formation and drag effect as the strain rate is increased. This explains the large upturn seen in Cu-1at.%Ta compared to Cu-5at.% Ta, owing to the less optimum microstructure to control the phonon drag or the time limiting SOC.

4. Discussion

Stabilizing the average grain size to the nano regime resulted in two important observations in this work that need thorough analysis, namely (1) no/delayed flow stress upturn as the strain rate is increased for smaller grain sizes, and (2) enhanced plasticity at high strain rate. Additionally, the nanocrystalline alloys were also observed to exhibit extraordinary quasi-static strength far beyond the contribution from grain boundary strengthening. For instance, nanocrystalline Cu-10at.%Ta possessed a room temperature strength of around 1.2 GPa of which the Hall-Petch contribution was about 400 MPa and other strengthening effects like the rule of mixtures were relatively less [25]. Thus, the secondary strengthening mechanism should account for the remaining ~67% of the strength. In fact, through atomistic simulations, authors have earlier revealed the main contribution of such exceptional strength to be the interaction of dislocations with Ta nanoclusters, which

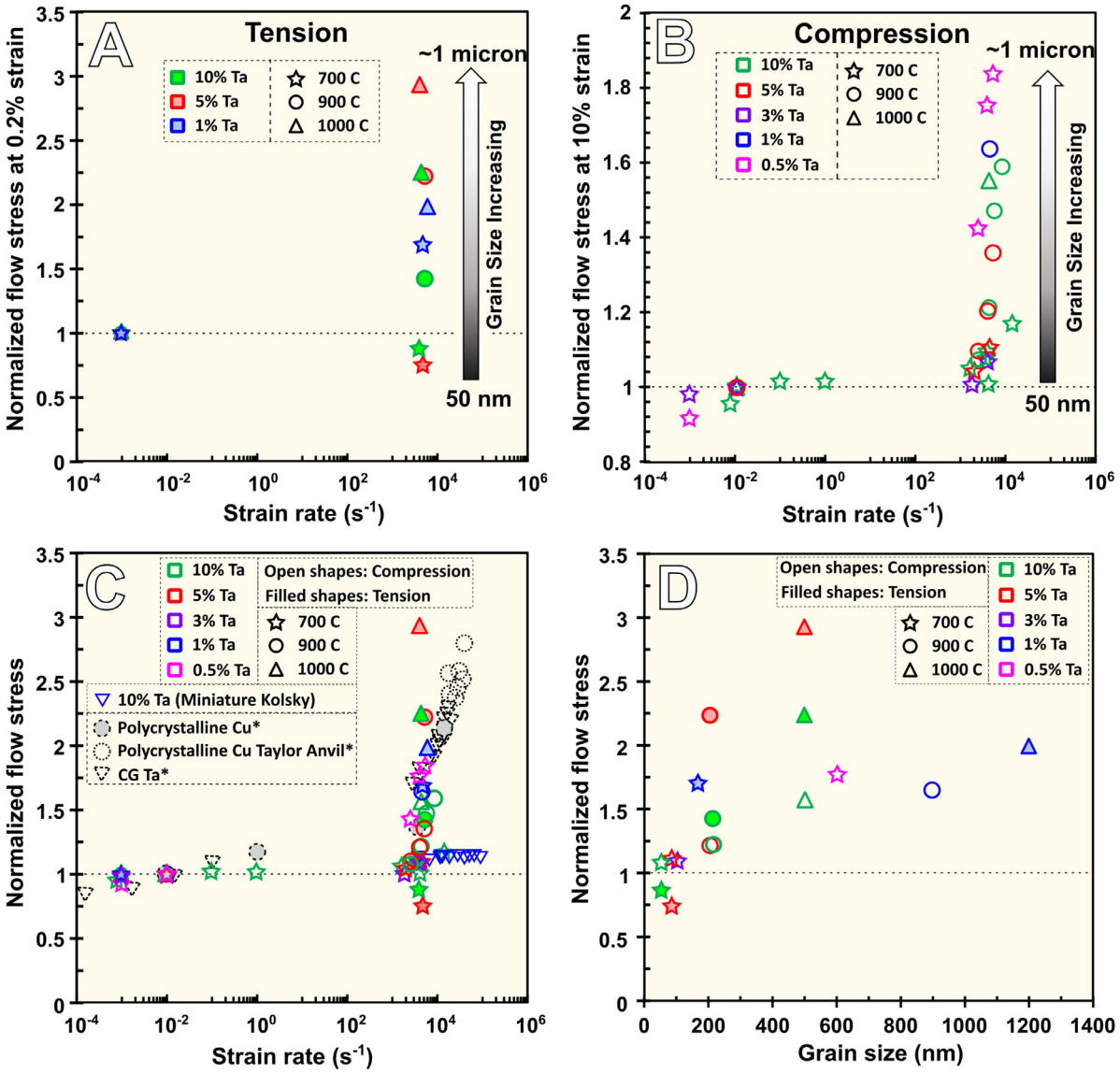

Fig. 3. Normalized flow stress as a function of (A) Strain rate in tension and (B) Strain rate in compression (C) Combined plot of tension (0.2%) and compression (10%) for various Cu-Ta samples (with literature data points for CG Cu and Ta [12]), (D) Grain size for both compression and tension at similar strain rate (~4000 /s).

was calculated to be around 800 MPa at room temperature [25], thus manifesting the significant role played by the nanoclusters in high strength of these alloys. In terms of high-strain rate behavior, the deformation mechanism causing flow stress upturn is a source of great debate [27–32]. The classical theory of dislocation drag mechanism is that dislocations moving freely through lattice experience a drag force from interactions with lattice vibrations when the dislocation is moving fast enough [30–32]. The drag force on the dislocation, in this case, can be represented simply by the expression $F = Bv$, where v is the average velocity of a mobile dislocation, and B is the drag coefficient, which is a function of material parameters and temperature. The drag coefficient, B, can be expressed as a summation of drag effects on the dislocation represented by

$$B = B_e + B_m + B_{ph} \tag{2}$$

where B_e is the coefficient of electron drag, which applies to metals tested below the Debye temperature (typically lower than room temperature testing), B_m is a drag co-efficient that only applies to magnetic or neo-magnetic metals, and B_{ph} is the coefficient of drag relating to interactions of mobile dislocations with phonons. This B_{ph} becomes predominant at high temperatures and high strain rates as observed in this work [31]. Further, drag effects will also increase as the volume fraction of interfaces/defects increases (i.e., in nano-grain materials) which is significant in that it results in an increase in phonon density of states and hence scattering [33]. Likewise, an increased phonon density of states has been calculated for nanocrystalline Cu-Ta alloys by the authors indicating phonon drag to be a potential operating mechanism [12]. On the other hand, the TEM microstructure showed limited dislocation avalanche in the nanocrystalline alloys indicating a limited contribution of SOC mechanism in NC alloys. Nevertheless, through both these mechanisms, the upturn in flow stress can be delayed if dislocations are prevented from reaching a maximum average velocity and forming SOCs, respectively, by pinning the dislocations at defects such as grain boundaries or Ta nanoclusters (eg., refer to Fig. 5). In the case of Cu-Ta alloys, this is more probable for alloys having a higher concentration of Ta solute and/or a lower processing temperature, wherein the barriers (grain boundaries and clusters) to dislocation glide are high (i.e. the average cluster spac-

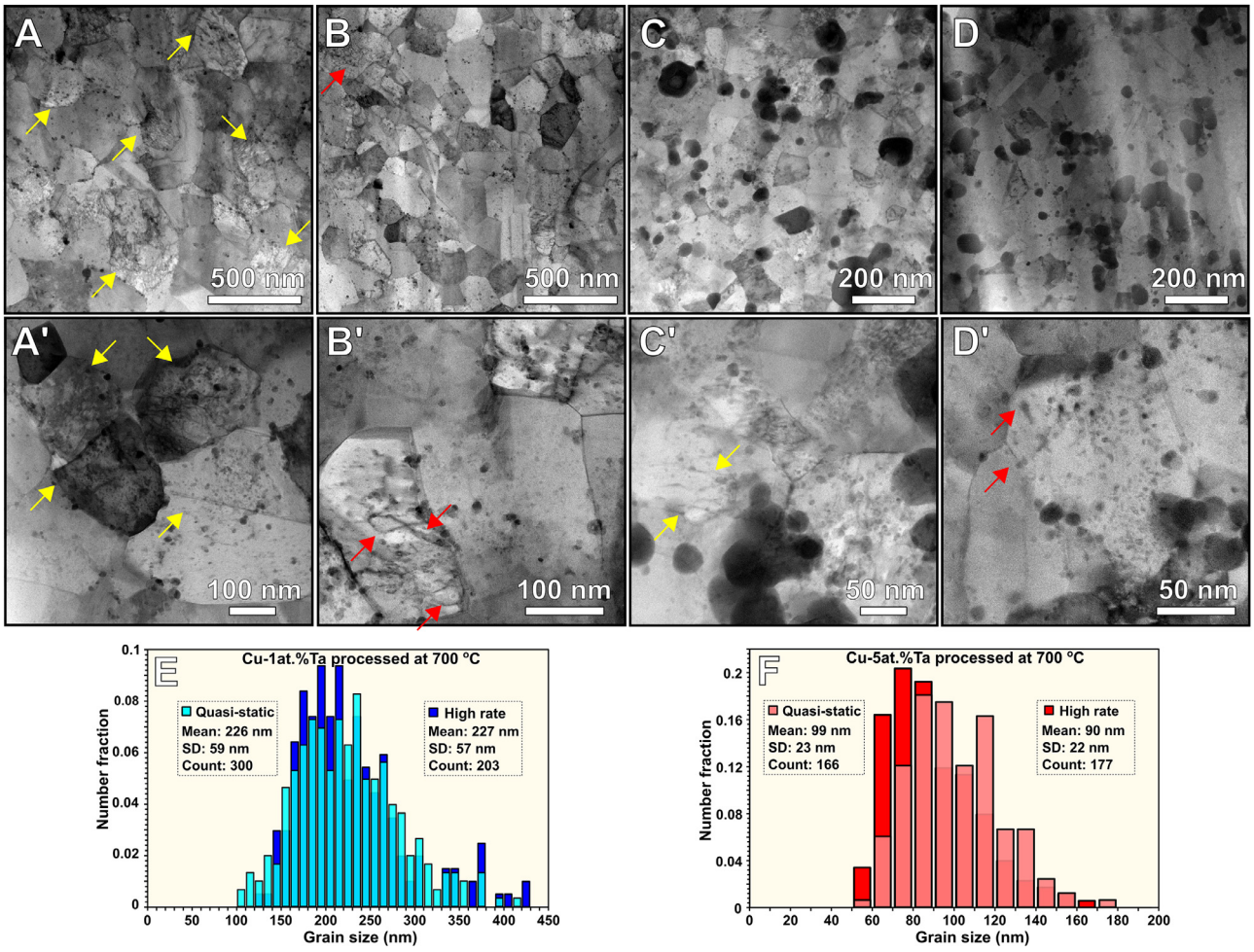

Fig. 4. Post deformed microstructure. BF STEM images of (A-A') Cu-1at.%Ta processed at 700°C and tested at quasi-static strain rate and (B-B') High strain rate; (C-C') Cu-5at.%Ta processed at 700°C and tested at quasi-static strain rate and (D-D') High strain rate; Dislocation activities are highlighted with yellow arrows in quasi-static and red arrows in high rate (E-F) Grain size distribution of post deformed Cu-1at.%Ta and Cu-5at.%Ta respectively.

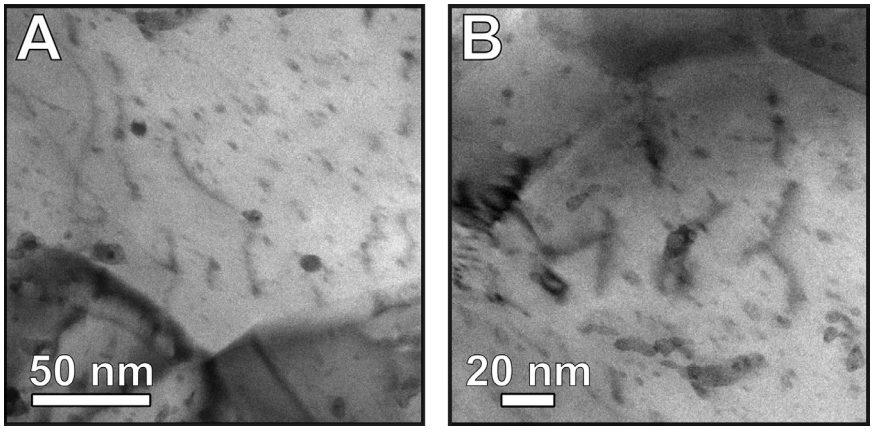

Fig. 5. Microstructural characterization of dislocation interaction with the precipitates. (A-B) BF-STEM images showing dislocations pinned by Ta nanoclusters in Cu-3at.%Ta processed at 700°C.

ing is small, ~ 4 nm [12]), thus keeping the flow stress within the range of thermal activation processes (i.e., nucleation). This holds true as long as the grain size lies below a critical size (~ 200 nm), where the nucleation of lattice dislocations becomes progressively frustrated and nucleation of dislocations at grain boundaries becomes more and more prevalent [34,35]. However, as grain size is increased, the probability or nucleation rate of dislocations within the lattice increases. This combined with factors that promote increased phase separation and coarsening of the Ta phases (e.g., higher temperatures), i.e., Ostwald ripening and decreased number fractions yield an increased average spacing of the Ta based clusters resulting in a higher probability of SOC formation and dislocations attaining a critical velocity at any given temperature. In fact, earlier atomistic work has shown that cluster spacing is criti-

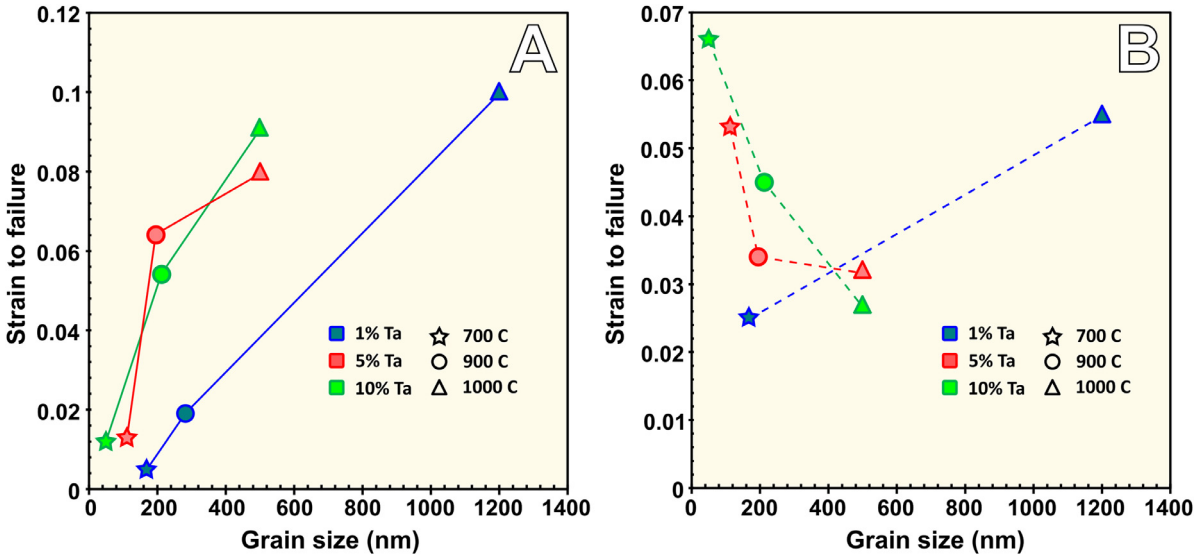

Fig. 6. Tensile ductility as a function of grain size for (a) quasi-static, and (b) high strain rate conditions. The Ta concentrations are color-coded with blue, red, and green corresponding to concentrations of 1at. %, 5 at.%, and 10at.%, respectively. The markers for each sample are denoted by the ☆, O, and Δ which correspond to samples processed at 700°C, 900°C, and 1000°C, respectively.

cal [12] and their change over the range of 5 nm to 15 nm is critical in determining what steady-state velocity can be attained or limited to [25] and if phonon drag effect and increased flow stress will be observed. Overall, there are two important aspects governing dynamic deformation behavior, namely, the dislocation nucleation rate and the dislocation pinning/unpinning process (an associated wait time). Both are critically controlled in Cu-Ta alloys by the Ta solute concentration and the overall processing temperature, which governs the grain size and Ta nanocluster spacing. Thus, as the grain size is reduced to below a critical level (more nano); materials tend to exhibit negligible strain rate sensitivity (due to pinning effects and lack of lattice nucleated dislocation) while maintaining the quasi-static strength. Note that the dislocations can still be nucleated from within the grain boundary regions; however, this volume is still limited relative to the lattice volume for grain sizes above 20 nm.

Further investigation into the effect of microstructure on enhanced tensile plastic behavior showed high tensile plasticity in coarse-grained Cu-Ta alloys (250 nm and beyond). This is expected since, in coarse-grained materials, it is easier to nucleate and store lattice dislocations leading to improved plasticity and lower strength at the quasi-static condition as compared to a higher strain-rate condition. While as the grain size is reduced, the volume fraction of the internal crystal region decreases and respectively so does the volume from which dislocation can be nucleated and stored. This is specifically true for nanograined materials where the pressure required to nucleate dislocations is relatively high, and the available volume to store dislocations is dictated by the limited grain boundary volume. This observed behavior is shown in Fig. 6A, where under quasi-static conditions, the tensile plasticity increased with an increase in the average grain size, with a consistent trend for all Ta concentrations. However, as the strain rate was increased, the exact opposite trend was observed for the alloys with an average grain size below 150 nm, as shown in Fig. 6B. For instance, Cu-10at.%Ta alloy processed at 700°C with an average grain size of 50 nm, exhibited the highest ductility of 6.5%. And as the processing temperature increased from 700°C to 1000°C, i.e., the average grain size increased from 50 nm to 600 nm, and the ductility dropped to 3%. Thus, there seems to be a critical average grain size (or range) (~150 nm), below which ductility at dynamic rates is enhanced. In NC materials, as the strain rate is increased, the grain boundary dislocations become more easily nucleated, i.e., a larger fraction of grain boundaries will participate in deformation at a high rate as compared to quasi-static conditions due to the increasing stress. Thus, the dynamic ductility is enhanced in NC materials. Interestingly, alloys with higher Ta concentrations exhibited better dynamic ductility for similar grain sizes. This aspect may be related to load transfer across the cluster matrix interface, resulting in delayed fracture initiation during dynamic loading, but will need to be analyzed in detail in a later study.

5. Conclusion

In summary, varying composition and processing temperatures of the Cu-Ta system allowed investigation of the separate effects of grain size and Ta particle distribution on the flow stress-strain rate response of the alloy. Increasing the processing temperature above 700°C was found to increase the grain size from the NC regime for concentrations of 5at.% and 10at.% Ta into the ultrafine-grained regime. Decreasing Ta concentration to 1at.% and 0.5at.% also allowed grain growth at 700°C into the ultrafine-grained regime, but the effect was less significant than an increase in processing temperature to 900°C for the 5at.% and 10at.%Ta materials. This shift from the nanocrystalline to the ultrafine grain regime is seen to be sufficient to cause the material to shift from a brittle failure to possessing a ductility of at least 4.5% plastic strain. Further, the NC material showed an increase in tensile ductility at high strain rates unlike the decrease in ductility observed in the ultrafine-grained metals at high rates. Furthermore, a comparison of the change of flow stress at high strain rates relative to that at a low strain rate revealed that a significant rise in flow stress is not observed in nanocrystalline metals. However, as the grain size increases and the Ta concentration reduces, the upturn in flow stress appears to become more significant. The greater of these effects appears to be the influence of grain size; however, Ta concentrations do play an important role in pinning the dislocations and therefore delaying the mechanisms controlling flow-stress upturn at higher strain rates. Likewise, tension-compression asymmetry was apparent in coarse-grained alloys, while it tends to be suppressed in nanocrystalline Cu-Ta alloys. Overall, the present work shows that there is a critical length scale, i.e., small grain size and appropriate clus-

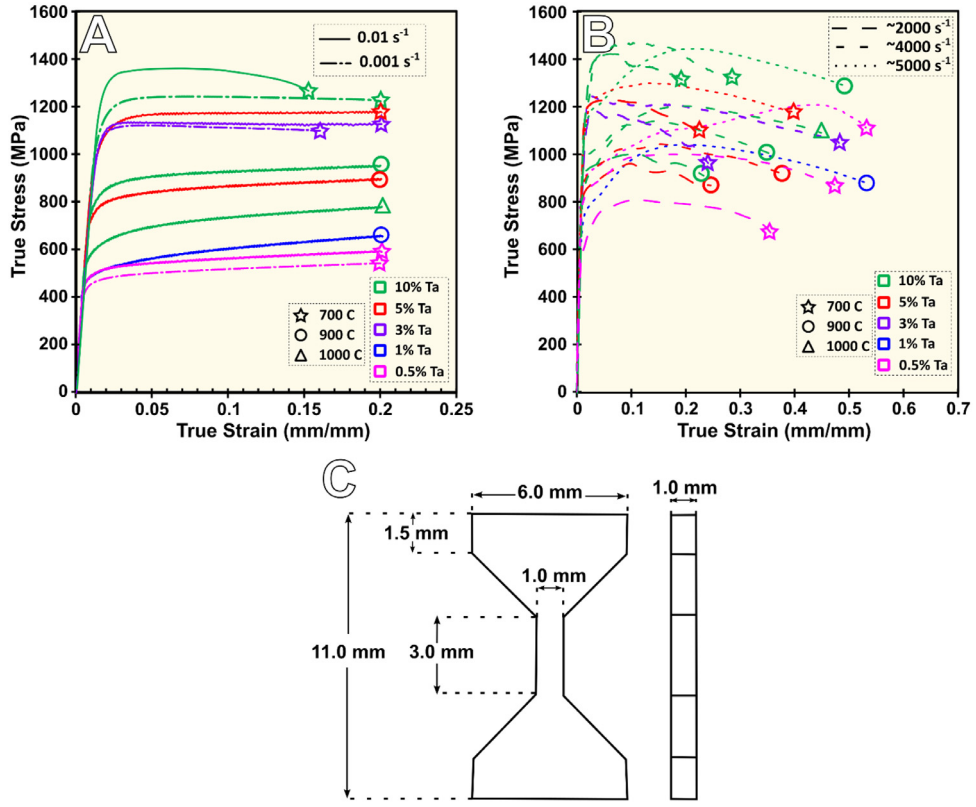

Fig. A1. (A&B) Compression stress strain response of all the alloys tested at quasi static and high strain rates, respectively. (C) Rectangular dog-bone tensile specimen dimensions.

ter spacing, below which flow stress upturn is damped out. This observation of changes in flow stress upturn phenomenon is consistent with the observed changes in measured plasticity or ductility, which enhances as the length-scale decreases below the critical length scale.

Data and materials availability

The data that support the findings are available from the corresponding authors upon request.

Declaration of Competing Interest

The authors declare no competing financial interests.

Acknowledgements

S.S., S.T., S.S., C.K., and K. S. acknowledge the use of facilities within the Eyring Materials Center at Arizona State University supported in part by NNCI-ECCS-1542160. The US Army Research Laboratory and the National Science Foundation under grants W911NF-15-2-0038 and 1663287 respectively supported this work.

Appendix

Fig. A1, Fig. A2, Fig. A3 and Table. A1.

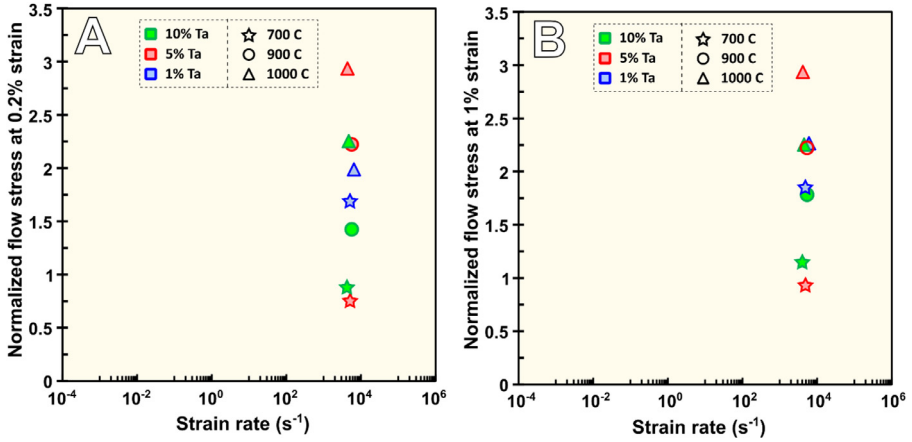

Fig. A2. Normalized tensile flow stress as a function of strain rate (A) 0.2% flow stress at high rate normalized with 0.2% at QSR (B) 1% flow stress at high rate normalized with 0.2% at QSR.

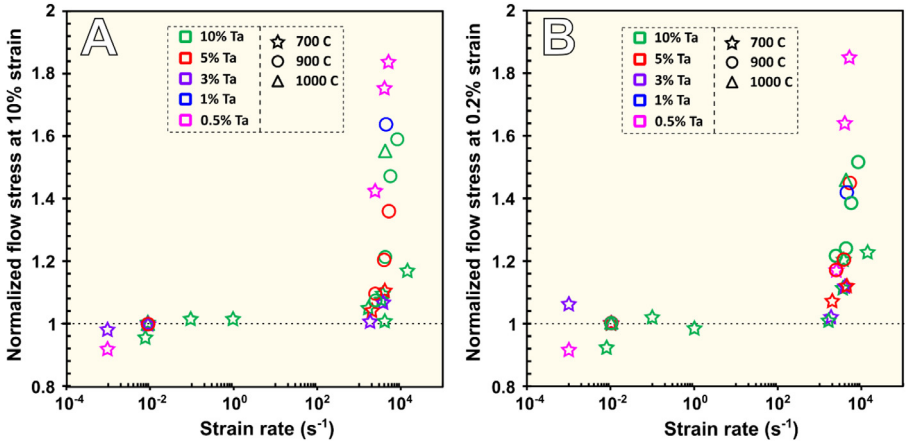

Fig. A3. Normalized compressive flow stress as a function of strain rate (A) 10% flow stress at high rate normalized with 10% at QSR (B) 0.2% flow stress at high rate normalized with 0.2% at QSR.

Table A1
Tensile flow stress results normalized for 1% strain at a high rate with 0.2% at quasi-static. Numbers in bracket indicate the order of increasing normalized flow stress from lowest to highest. This is compared with the corresponding values at high strain rate normalized at 0.2% strain.

Ta at. %	Processing T (°C)	Strain rate (s^{-1})	1%Normalized flow stress	0.2% normalized
Cu 1 at.% Ta	700	0.001	-	
		4950	1.84 (4)	1.71 (4)
	1000	0.001	-	-
		6300	2.25 (7)	2.0 (5)
Cu 5 at.% Ta	700	0.001	-	-
		4990	0.91 (1)	0.75 (1)
	900	0.01	-	-
		5500	2.24 (5)	2.24 (6)
	1000	0.001	-	-
		4200	2.93 (8)	2.93 (8)
Cu 10 at.% Ta	700	0.001	-	-
		4100	1.13 (2)	0.88 (2)
	900	0.001	-	-
		5500	1.79 (3)	1.43 (3)
	1000	0.001	-	-
		4500	2.24 (6)	2.24 (7)

References

[1] M.A. Meyers, Dynamic behavior of materials, John wiley & sons, 1994.
[2] D. Jia, Y.M. Wang, K.T. Ramesh, E. Ma, Y.T. Zhu, R.Z. Valiev, Deformation behavior and plastic instabilities of ultrafine-grained titanium, Appl. Phys. Lett. 79 (2001) 611–613, doi:10.1063/1.1384000.
[3] D.R. Chichili, K.T. Ramesh, K.J. Hemker, The high-strain-rate response of alpha-titanium: experiments, deformation mechanisms and modeling, Acta Mater 46 (1998) 1025–1043, doi:10.1016/S1359-6454(97)00287-5.
[4] D. Jia, K.T. Ramesh, E. Ma, Effects of nanocrystalline and ultrafine grain sizes on constitutive behavior and shear bands in iron, Acta Mater. 51 (2003) 3495–3509, doi:10.1016/S1359-6454(03)00169-1.
[5] F. Dalla Torre, H. Van Swygenhoven, M. Victoria, Nanocrystalline electrodeposited Ni: microstructure and tensile properties, Acta Mater. 50 (2002) 3957–3970, doi:10.1016/S1359-6454(02)00198-2.
[6] P.S. Follansbee, G. Regazzoni, U.F. Kocks, Mechanical properties at high rates of strain, in: Proc. Third Conf. Mech. Prop. Mater. High Rates Strain, 1984, pp. 9–12.
[7] J. Hirth, J. Lothe, in: Theory of Dislocations, McGraw-Hill, New York, 1968, p. 780.
[8] Y. Fan, Y. Osetsky, S. Yip, B. Yildiz, Onset mechanism of strain-rate-induced flow stress upturn, Phys. Rev. Lett. 109 (2012) 135503, doi:10.1103/PhysRevLett.109.135503.
[9] A.Y. Kuksin, A.V. Yanilkin, Atomistic simulation of the motion of dislocations in metals under phonon drag conditions, Phys. Solid State 55 (2013) 1010–1019, doi:10.1134/S1063783413050193.
[10] X. Chen, L. Xiong, D.L. McDowell, Y. Chen, Effects of phonons on mobility of dislocations and dislocation arrays, Scr. Mater. 137 (2017) 22–26, doi:10.1016/j.scriptamat.2017.04.033.
[11] L. Lea, L. Brown, A. Jardine, Time limited self-organised criticality in the high rate deformation of face centred cubic metals, Commun. Mater. 1 (2020) 93, doi:10.1038/s43246-020-00090-2.
[12] S.A. Turnage, M. Rajagopalan, K.A. Darling, P. Garg, C. Kale, B.G. Bazehhour, I. Adlakha, B.C. Hornbuckle, C.L. Williams, P. Peralta, K.N. Solanki, Anomalous mechanical behavior of nanocrystalline binary alloys under extreme conditions, Nat. Commun. 9 (2018), doi:10.1038/s41467-018-05027-5.
[13] D. Casem, J. Ligda, T. Walter, K. Darling, B. Hornbuckle, Strain-rate sensitivity of nanocrystalline Cu–10Ta to 700,000/s, J. Dyn. Behav. Mater. (2019), doi:10.1007/s40870-019-00223-w.
[14] Q. Wei, S. Cheng, K.. Ramesh, E. Ma, Effect of nanocrystalline and ultrafine grain sizes on the strain rate sensitivity and activation volume: fcc versus bcc metals, Mater. Sci. Eng. A 381 (2004) 71–79, doi:10.1016/j.msea.2004.03.064.
[15] M. Rajagopalan, K. Darling, S. Turnage, R. Koju, B. Hornbuckle, Y. Mishin, K. Solanki, Microstructural evolution in a nanocrystalline Cu-Ta alloy: a combined in-situ TEM and atomistic study, Mater. Des. 113 (2017) 178–185.
[16] B.C. Hornbuckle, T. Rojhirunsakool, M. Rajagopalan, T. Alam, G.P. Purja Pun, R. Banerjee, K.N. Solanki, Y. Mishin, L.J. Kecskes, K.A. Darling, Effect of Ta solute concentration on the microstructural evolution in immiscible Cu-Ta alloys, JOM 67 (2015) 2802–2809, doi:10.1007/s11837-015-1643-x.
[17] V.H. Hammond, T.L. Luckenbaugh, M. Aniska, D.M. Gray, J.A. Smeltzer, B.C. Hornbuckle, C.J. Marvel, K.N. Solanki, T. Schmitz, K.A. Darling, An insight into machining of thermally stable bulk nanocrystalline metals, Adv. Eng. Mater. 20 (2018) 1800405, doi:10.1002/adem.201800405.
[18] C. Kale, M. Rajagopalan, S. Turnage, B. Hornbuckle, K. Darling, S.N. Mathaudhu, K.N. Solanki, On the roles of stress-triaxiality and strain-rate on the deformation behavior of AZ31 magnesium alloys, Mater. Res. Lett. 6 (2018) 152–158, doi:10.1080/21663831.2017.1417923.
[19] C. Kale, S. Turnage, D.Z. Avery, H.El Kadiri, J.B. Jordon, K.N. Solanki, Towards dynamic tension-compression asymmetry and relative deformation mechanisms in magnesium,, Materialia 9 (2020) 100543, doi:10.1016/j.mtla.2019.100543.
[20] D.J. Barton, C. Kale, B.C. Hornbuckle, K.A. Darling, K.N. Solanki, G.B. Thompson, Microstructure and dynamic strain aging behavior in oxide dispersion strengthened 91Fe-8Ni-1Zr (at%) alloy, Mater. Sci. Eng. A 725 (2018) 503–509, doi:10.1016/j.msea.2018.04.016.

[21] B.A. Gama, S.L. Lopatnikov, J.W. Gillespie, Hopkinson bar experimental technique: a critical review, Appl. Mech. Rev. 57 (2004) 223–250, doi:10.1115/1.1704626.
[22] C. Kale, S. Srinivasan, B.C. Hornbuckle, R.K. Koju, K. Darling, Y. Mishin, K.N. Solanki, An experimental and modeling investigation of tensile creep resistance of a stable nanocrystalline alloy, Acta Mater. 199 (2020) 141–154, doi:10.1016/j.actamat.2020.08.020.
[23] K.A. Darling, M. Rajagopalan, M. Komarasamy, M.A. Bhatia, B.C. Hornbuckle, R.S. Mishra, K.N. Solanki, Extreme creep resistance in a microstructurally stable nanocrystalline alloy, Nature 537 (2016) 378–381, doi:10.1038/nature19313.
[24] M. Rajagopalan, K.A. Darling, C. Kale, S.A. Turnage, R.K. Koju, B.C. Hornbuckle, Y. Mishin, K.N. Solanki, Nanotechnology enabled design of a structural material with extreme strength as well as thermal and electrical properties, Mater. Today 31 (2019) 10–20, doi:10.1016/j.mattod.2019.09.024.
[25] C. Kale, S. Turnage, P. Garg, I. Adlakha, S. Srinivasan, B.C. Hornbuckle, K. Darling, K.N. Solanki, Thermo-mechanical strengthening mechanisms in a stable nanocrystalline binary alloy – a combined experimental and modeling study, Mater. Des. 163 (2019) 107551, doi:10.1016/j.matdes.2018.107551.
[26] R.K. Koju, K.A. Darling, K.N. Solanki, Y. Mishin, Atomistic modeling of capillary-driven grain boundary motion in Cu-Ta alloys, Acta Mater. 148 (2018) 311–319, doi:10.1016/j.actamat.2018.01.027.
[27] G. Regazzoni, U.F. Kocks, P.S. Follansbee, Dislocation kinetics at high strain rates, Acta Metall. 35 (1987) 2865–2875, doi:10.1016/0001-6160(87)90285-9.
[28] P.S. Follansbee, U.F. Kocks, A constitutive description of the deformation of copper based on the use of the mechanical threshold stress as an internal state variable, Acta Metall. 36 (1988) 81–93, doi:10.1016/0001-6160(88)90030-2.
[29] P.S. Follansbee, J. Weertman, On the question of flow stress at high strain rates controlled by dislocation viscous flow, Mech. Mater. 1 (1982) 345–350, doi:10.1016/0167-6636(82)90034-5.
[30] A. Kumar, R.G. Kumble, Viscous drag on dislocations at high strain rates in copper, J. Appl. Phys. 40 (1969) 3475–3480, doi:10.1063/1.1658222.
[31] E. Nadgornyi, Dislocation dynamics and mechanical properties of crystals, Prog. Mater. Sci. 31 (1988) 1–530, doi:10.1016/0079-6425(88)90005-9.
[32] R.F. Smith, J.H. Eggert, R.E. Rudd, D.C. Swift, C.A. Bolme, G.W. Collins, High strain-rate plastic flow in Al and Fe, J. Appl. Phys. 110 (2011) 123515, doi:10.1063/1.3670001.
[33] D. Şopu, J. Kotakoski, K. Albe, Finite-size effects in the phonon density of states of nanostructured germanium: A comparative study of nanoparticles, nanocrystals, nanoglasses, and bulk phases, Phys. Rev. B 83 (2011) 245416, doi:10.1103/PhysRevB.83.245416.
[34] H. Van Swygenhoven, P.M. Derlet, A.G. Frøseth, Nucleation and propagation of dislocations in nanocrystalline fcc metals, Acta Mater. 54 (2006) 1975–1983, doi:10.1016/j.actamat.2005.12.026.
[35] V. Yamakov, D. Wolf, S.R. Phillpot, A.K. Mukherjee, H. Gleiter, Deformation-mechanism map for nanocrystalline metals by molecular-dynamics simulation, Nat. Mater. 3 (2004) 43–47, doi:10.1038/nmat1035.